Heterogeneity of Chloride Channels in the Apical Membrane of Isolated Mitochondria-rich Cells from Toad Skin

J. BALSLEV SØRENSEN and E. HVIID LARSEN

From the August Krogh Institute, The University of Copenhagen, Universitetsparken 13, DK-2100 Copenhagen Ø, Denmark

ABSTRACT The isolated epithelium of toad skin was disintegrated into single cells by treatment with collagenase and trypsine. Chloride channels of cell-attached and excised inside-out apical membrane-patches of mitochondria-rich cells were studied by the patch-clamp technique. The major population of Cl^- channels constituted small 7-pS linear channels in symmetrical solutions (125 mM Cl^-). In cell-attached and inside-out patches the single channel *i/V*-relationship could be described by electrodiffusion of Cl^- with a Goldmann-Hodgkin-Katz permeability of, $P_{Cl} = 1.2 \times 10^{-14} - 2.6 \times 10^{-14}$ cm$^3 \cdot$ s^{-1}. The channel exhibited voltage-independent activity and could be activated by cAMP. This channel is a likely candidate for mediating the well known cAMP-induced transepithelial Cl^- conductance of the amphibian skin epithelium. Another population of Cl^- channels exhibited large, highly variable conductances (upper limit conductances, 150–550 pS) and could be activated by membrane depolarization. A group of intermediate-sized Cl^--channels included: (*a*) channels (mean conductance, 30 pS) with linear or slightly outwardly rectifying *i/V*-relationships and activity occurring in distinct "bursts," (*b*) channels (conductance-range, 10–27 pS) with marked depolarization-induced activity, and (*c*) channels with unresolvable kinetics. The variance of current fluctuations of such "noisy" patches exhibited a minimum close to the equilibrium-potential for Cl^-. With channels occurring in only 38% of sealed patches and an even lower frequency of voltage-activated channels, the chloride conductance of the apical membrane of mitochondria-rich cells did not match quantitatively that previously estimated from macroscopic Ussing-chamber experiments. From a qualitative point of view, however, we have succeeded in demonstrating the existence of Cl^-channels in the apical membrane with features comparable to macroscopic predictions, i.e., activation of channel gating by cAMP and, in a few patches, also by membrane depolarization.

KEY WORDS: patch clamp • epithelial chloride channels • cyclic AMP • amphibian skin

INTRODUCTION

The existence of minority cell types with supposed functions in ion transport is a collective property of a number of tight epithelia including amphibian skin and distal renal epithelia of vertebrates. For example, the mitochondria-rich (MR)[1] cells of toad and frog skin have been assigned a number of distinct functions including acid secretion by apical proton pumps (Page and Frazier, 1987; Ehrenfeld et al., 1989; Larsen et al., 1992), sodium absorption via apical amiloride-sensitive channels and basolateral Na/K-ATPases (Larsen et al., 1987; Harvey, 1992; Rick, 1992), and active as well as passive Cl^--uptake (Voûte and Meier, 1978; Larsen, 1991; Rick, 1994).

The localization of a voltage-dependent Cl^- transport to MR-cells was originally based on the correlation between conductive Cl^- fluxes and the number of MR-cells in the skin (Voûte and Meier, 1978; Willumsen and Larsen, 1986; Devuyst et al., 1991). Also other observations indicated that the Cl^- conductance was cellular rather than paracellular. The elimination of Na^+ transport by amiloride or by exposure to an Na^+-free apical solution reduced the conductive unidirectional Cl^- fluxes in the short-circuited skin indicating that a Cl^- conductance is colocalized with an Na^+ conductance in the apical membrane (Kristensen, 1978; 1983). Other studies showed that arginin vasotocin, which activates the apical Na^+ conductance of principal cells, failed to co-activate the Cl^--flux (Kristensen, 1981) and that the apical membrane of principal cells remained tight for Cl^- even in skins with a fully voltage- (Willumsen and Larsen, 1986) or cAMP- (Willumsen et al., 1992) activated Cl^- conductance. These results indicated that the principal cells do not conduct transepithelial Cl^- currents. Another line of evidence established that the apical membrane of MR-cells is permeable to Cl^-. When challenged with a Cl^--containing apical solution and sufficient K^+ in the serosal solution, MR-cells swelled with the activation of the transepithelial Cl^- conductance indicating that Cl^- can enter MR-cells through the apical membrane (Voûte and Meier, 1978; Foskett and Ussing, 1986; Larsen et al., 1987). Chloride

Portions of this study have been previously presented in abstract form (Sørensen, J.B., and E.H. Larsen. 1995. *J. Physiol. (Lond.).* 482:8P; and Sørensen, J.B., and E.H. Larsen. 1995. *J. Physiol. (Lond.).* 489:116P).

Address correspondence to Jakob Balslev Sørensen, August Krogh Institute, Universitetsparken 13, DK-2100 Copenhagen Ø, Denmark; Fax: 45-3532-1567; E-mail: JBSorensen@aki.ku.dk

[1] *Abbreviations used in this paper:* CFTR, cystic fibrosis transmembrane conductance regulator; GHK, Goldman-Hodgkin-Katz; MR-cell, mitochondria-rich cell.

J. GEN. PHYSIOL. © The Rockefeller University Press • 0022-1295/96/11/421/13 $2.00
Volume 108 November 1996 421–433

currents originating from MR-cells were measured with the vibrating voltage-electrode (Foskett and Ussing, 1986; Katz and Scheffey, 1986), and using the electron microprobe technique Rick (1994) demonstrated Br^- entry in MR-cells from the outer solution.

The above two lines of evidence demonstrate, on the one hand, that the transepithelial Cl^- conductance is cellular but not localized to principal cells and, on the other, that MR-cells harbor an apical Cl^- conductance. With this information, and because of the obvious difficulties in accessing directly the MR-cells with microelectrodes, we now generally assume that properties of the MR-cell Cl^- conductance can be inferred from Ussing-chamber experiments. Recently, a method for studying isolated MR-cells suspended in a Ringer solution was developed which allows for application of patch-clamp methods to individual cells (Larsen and Harvey, 1994). It is now possible to investigate directly ion channels expressed in MR-cells in their own right, as well as addressing the basic assumption that the MR-cell Cl^- conductance constitutes the physiological pathway for transepithelial Cl^- uptake. Using this technique we here report on properties of individual Cl^- channels of the apical membrane of toad skin MR-cells.

MATERIALS AND METHODS

Preparation of Isolated Mitochondria-rich Cells

Toads (*Bufo bufo*) were kept at room temperature and fed mealworms once a week. 5–10 d before use the toads were transferred to trays with 1–2 cm 0.1 M $NaNO_3$ or, in few experiments, with distilled H_2O. The treatment with Cl^--free external solution increases the number of MR-cells (Katz and Gabbay, 1988) and the apical area per cell, thus facilitating the study of the apical membrane. Untreated animals were often found to have so few MR-cells and/or so small an apical membrane area that patch-clamp studies were unfeasible. The animals were killed by decapitation and pithing. MR-cells were prepared from the isolated skin epithelium by a method slightly modified from that of Larsen and Harvey (1994). Briefly, the epithelium was isolated by ~2 h serosal exposure of the whole skin to 2 mg ml^{-1} crude collagenase (cat. no. 103586; Boehringer-Mannheim GmbH, Mannheim, Germany) in standard Ringer (see *Solutions*). The isolated epithelium was bilaterally treated for 1 h by 2 mg ml^{-1} Collagenase A1 (C9891; Sigma Chemical Co., St. Louis, MO) in standard Ringer. After washing the epithelium twice in Ca^{2+}-free Ringer, it was put through sequential 3-min treatments of 0.1 mg/ml trypsin (17072-018, Trypsin 1:250 USP grade; Life Technologies Ltd., Paisley, UK) in Ca^{2+}-free Ringer, resulting in 5–10 fractions of isolated epithelial cells. Each fraction was immediately diluted 10:1 by standard Ringer (1 mM Ca^{2+}) and centrifuged at 800–900 rpm for 5 min. The cell pellet was resuspended in 1 ml modified Ringer (see *Solutions*) and the cells were then ready to use. With the above isolation procedure, we found that the MR-cells were most frequent in fractions No. 7–9.

Single-channel Patch-clamp

Micropipettes were fabricated from borosilicate glass tubes with inner filament (GC150F-15, Clark Electromedical Instruments, Reading, UK) on a horizontal DMZ-puller (Zeitz Instruments, Augsburg, Germany). After heat-polishing, the tip resistance of the patch electrodes was ~8–12 MΩ measured with modified Ringer in pipette and bath. A sample of cells was suspended in ~1 ml modified Ringer in a Petri dish (4 cm OD; Nunc, Roskilde, Denmark) and placed on the stage of an inverted microscope (Zeiss IM35; Brock & Michelsen, Birkerød, Denmark). Viewed with Nomarski optics at 400× magnification, MR-cells were easily recognized by their distinct flask-shape which is retained after isolation (Larsen and Harvey, 1994). On some but not all MR-cells, the apical membrane was clearly visible as an apical concavity surrounded by a ridge. With a micromanipulator (WR-90; Narishige, Tokyo, Japan) the tip of the patch electrode was directed to the apical concavity of such cells. Seals were formed either immediately or after very slight suction. However, the study of single channels was hampered by, (*a*) a very low frequency of gigaseal formation (probably <5%), (*b*) a low resistance of obtained gigaseals (~10 GΩ in most cases, but often seals with a lower resistance were also accepted), and (*c*) short life times of patches, i.e., the majority of patches lasted for <10 min. Thus, as is often the case with native epithelial cells, the seals obtained on the apical membrane of MR-cells are very fragile. All experiments were done at room temperature (20–22°C), and channels were studied in both cell-attached and excised inside-out configurations.

Single Channel Current Recording

Voltage-clamp and current recordings of membrane patches were performed with an RK300-amplifier furnished with a 10 GΩ feedback-resistor in the headstage (gain 100 or 200 mV/pA; Biologic, Claix, France). Currents were recorded on VCR videotape at 20 kHz bandwidth (Panasonic AG-6200; Osaka, Japan) after pulse-code modulation (PCM-501es; Sony, Tokyo, Japan). For analysis, currents were played back, low-pass filtered at 100 or 200 Hz (f_c [−3 dB], 8-pole Butterworth; Frequency Devices, Inc., Haverhill, MA) and digitized at 1 or 2 kHz through a CED 1401 interface (output range, ±2.5 V, 12 bit resolution; Cambridge Electronic Design, Cambridge, UK). The CED patch- and voltage-clamp software (Version 6.2; Cambridge Electronic Design) was used for controlling clamping voltages and for digitizing and analyzing clamping currents.

Solutions

Standard Ringer (used for cell isolation) contained (mM): 116 Na^+, 3.7 K^+, 1 Ca^{2+}, 118.7 Cl^-, 4 SO_4^{2-}, 3 acetate, 11 glucose, 8 Tris (pH = 7.4). Ca^{2+}-free Ringer (used for cell isolation): 116 Na^+, 3.7 K^+, 116.7 Cl^-, 4 SO_4^{2-}, 3 acetate, 11 glucose, 10 EGTA, 8 Tris (pH = 7.4). Modified Ringer (used for cell isolation and as bath): 116 Na^+, 3.7 K^+, 4 Ca^{2+}, 124.7 Cl^-, 4 SO_4^{2-}, 3 acetate, 11 glucose, 8 Tris (pH = 7.2). Unless otherwise stated, the bath and pipette solutions for patch-clamp studies were modified Ringer with 100 μM amiloride added to the pipette solution. For verifying Cl^- selectivity of the channels in inside-out patches, a gravity-driven perfusion system was used to exchange the bath solution around the patch. A suction device placed in the Petri dish opposite to the place of solution delivery allowed for exchange of the entire bath solution. The solution used for perfusion in most cases contained 25 mM Cl^-, thus displacing the Nernst potential for Cl^- (E_{Cl}) from 0 to −40.6 mV (bath with reference to the pipette). Perfusion-solution: 140 *N*-methyl-D-glucamin ($NMDG^+$), 115 gluconate, 10 Na^+, 25 Cl^-, 1.63 Ca^{2+}, 1.14 Mg^{2+}, 5 EGTA (resulting free [Ca^{2+}] = 100 nM, [Mg^{2+}] = 1 mM), 10 *N*-tris(hydroxymethyl) methyl-2-aminoethane sulfonic acid (TES) (pH 7.2). Occasionally, patches were perfused with a solution in which $NMDG^+$ was replaced by 130 mM $Tris^+$ with 25 or 44 mM Cl^- and gluconate as the nonpermeant anion. Free-[Ca^{2+}] was 100 nM, and free-[Mg^{2+}] was 1 or 2 mM. ATP (A-0770) and for-

skolin (F-6886) were purchased from Sigma Chemical Co.; cAMP-dependent protein kinase (catalytic subunit) was purchased from Promega Corp. (V5221; Madison, WI) and added as stated.

Correction for Liquid Junction Potentials

Liquid junction potentials were measured between solutions that came into contact with each other during the experiment. With different solutions in pipette and bath (when *N*-methyl-D-glucamine in the pipette was occasionally substituted for Na^+) the membrane-potential, V_M, is given by the following (Neher, 1992),

$$V_M = V_c - V + V_{LJ}, \quad (1)$$

where V_c is the spontaneous membrane potential (zero for inside-out patches), V_{LJ} is the liquid junction potential (measured as bath relative to pipette), and V is the clamp-potential measured relative to the zero-current potential obtained by nulling external potential-offsets before the experiment. When, during an inside-out experiment, the original solution (1) is exchanged for another solution (2) a liquid junction-potential appears at the reference-electrode (0.15 M KCl bridge in our case) with the resulting membrane potential given by (Neher, 1992),

$$V_M = -V + V_{LJ} + V_{2,1}, \quad (2)$$

where $V_{2,1}$ is the potential of solution 2 with reference to solution 1. The liquid junction potentials were measured following Neher (1992), with the patch-clamp amplifier itself being used for generating a potential nulling the V_{LJ} between a pipette and bath solution. The zero-current potential was obtained by starting with the same test-solution in pipette and bath. The bath was then exchanged for the other (reference) solution and the potential generated by the amplifier in zero-current clamp mode (I_o) was noted as, $-V_{LJ}$. Finally, replacement of the original bath solution provided a check for reversibility. Each determination was done 6 times, and the mean was used for correcting expected reversal potentials, as indicated (individual data-points of the *i/V*-relationships were not corrected). All measurements were reversible within 0.6 mV. Junction potentials of relevance for the present study are given in Table I.

Currents through Individual Chloride Channels

With $[Cl^-]_c < [Cl^-]_o$, outward rectification of the chloride current (I_{Cl}) is expected from electrodiffusion under constant-field assumptions according to the Goldman-Hodgkin-Katz (GHK) equation (Goldman, 1943; Hodgkin and Katz, 1949),

$$I_{Cl} = P_{Cl} \cdot \frac{F^2 \cdot V_M}{R \cdot T} \cdot \frac{[Cl^-]_c - [Cl^-]_o \cdot \exp\{-F \cdot V_M/(R \cdot T)\}}{1 - \exp\{-F \cdot V_M/(R \cdot T)\}}, \quad (3)$$

TABLE I

Liquid Junction Potentials

Solution 1	Solution 2	$V_{2,1}$
Modified Ringer	Perfusion sol.	-2.7 ± 0.1 mV ($n = 6$)
NMDG-Ringer	Modified Ringer	-4.4 ± 0.3 mV ($n = 6$)

Liquid-junction potentials measured between Modified Ringer and the perfusion solution (*see Solutions*) and between Modified Ringer and NMDG-Ringer, where Na^+ was replaced by equimolar concentration of $NMDG^+$. The potential is given as solution 2 referenced to solution 1. Mean ± SEM is indicated.

where P_{Cl} is the permeability coefficient, V_M is the membrane potential, and F, R, and T have their usual meanings. Larsen and Harvey (1994) found that a subpopulation of MR-cells was characterized by whole-cell I_{Cl}/V-relationships that were well described by Eq. 3, whereas another subpopulation exhibited "instantaneous rectification" in that the instantaneous I_{Cl}/V-relationship rectified in excess of Eq. 3. Since, in a homogeneous population of ion channels, $I = i \cdot N \cdot P_o$, where I is the macroscopic current, i the single-channel current, N the number of channels, and P_o their open-probability, rectification of I in excess of Eq. 3 could be caused by either the single channel i/V-relationship being outwardly rectifying or P_o increasing with voltage (voltage activation). To investigate whether single Cl^- channels of the present study could be involved in one or the other kind of rectification, Eq. 3 was fitted to i/V-plots of currents through individual Cl^--channels. In cell-attached patches where, $V_M = V_c - V$ (assuming $V_{LJ} = 0$), V_c, $[Cl^-]_c$ and P_{Cl} were allowed to vary during the fit. In order to compare conductances obtained under different conditions, the conductance in symmetrical 125-mM Cl^- solutions ($\gamma_{125/125}$), when not measured directly, was calculated from P_{Cl} obtained by the GHK-fit according to,

$$\gamma_{C/C} = \frac{F^2}{RT} \cdot P_{Cl} \cdot [Cl^-], \quad (4)$$

where $[Cl^-] = 125$ mM. Similarly, the integral conductance at the reversal potential, γ_{rev}, can be calculated as (Sten-Knudsen, 1978),

$$\gamma_{rev} = \frac{F^3}{(RT)^2} \cdot \frac{[Cl^-]_o \cdot [Cl^-]_c}{[Cl^-]_c - [Cl^-]_o} \cdot P_{Cl} \cdot E_{Cl}, \quad (5)$$

where, $E_{Cl} = (RT/-F) \cdot \log_e([Cl^-]_o/[Cl^-]_c)$ is the equilibrium potential.

Analysis of Variance of Current Fluctuations

To evaluate the current variance in patches where single-channel levels could not be distinguished in all-points histograms, currents were redigitized using the SPAN-software program (J. Dempster, Strathclyde Electrophysiology, Glasgow, UK). Currents were amplified 10×, filtered at $f_c = 500$ Hz, and digitized at 1 kHz. The variance was calculated in blocks of 1,024 points and the mean between blocks used as the estimated variance.

RESULTS

Heterogeneity of Chloride Channels in the Apical Membrane

From the appearance of a single Lorentzian function in power spectra of stationary MR-cell current fluctuations it was concluded that the major voltage-activated Cl^--current was carried by a single population of large (~250 pS) channels with fast gating kinetics (mean corner-frequency, $f_c = 35$ Hz; Larsen & Harvey, 1994). It was hypothesized that this population of Cl^--selective channels was localized in the apical membrane, thus governing the voltage-activated influx of Cl^- from the external bath. In the present study of single Cl^- channels resolved in apical membrane patches, we unexpectedly found a marked heterogeneity of channels (Table II). The majority of Cl^- channels were small (7–8 pS) with a linear i/V-relationship under symmetrical conditions. A large channel corresponding to expectations from the above mentioned whole-cell analysis was

TABLE II

Electrical Activity of Membrane Patches

Patch type	Fraction
Silent	62%
Small linear Cl^- channel	26%
Giant Cl^- channel	3%
Intermediate Cl^- channel	10%
Unresolved kinetics	4%
TOTAL	100% (n = 179)
Too noisy for analysis	n = 45

Heterogeneity of patches obtained on the apical membrane of MR-cells. Percentages do not sum to 100% since more than one type of channel could be present in a patch. 45 patches had to be disregarded because the noise-level did not allow for analysis (not included in the total of 179).

observed in the present study, however, only occasionally. Furthermore, a number of channels of intermediate conductance were also found, some with kinetics unresolvable with our experimental setup. Patches with low seal resistances (MATERIALS AND METHODS) were often quite noisy and had to be discarded from the analysis.

Small Linear Chloride Channels (26% of the Patches)

Cell-attached configuration. The current-recordings shown in Fig. 1 are from a channel with relatively short openings at pipette potentials, $-V_p \neq 0$ mV. The amplitude of current transitions at different pipette potentials was estimated using Gaussian fits to all-points histograms and displayed as a function of $-V_p$. The channel currents shown in Fig. 1 reversed near zero mV indicating that the permeant ion was in equilibrium at the cell membrane potential. This is as expected for a Cl^- channel (Larsen et al., 1987). In agreement with this notion, the *i/V*-relationship exhibited slight outward rectification and could be fitted with the GHK-equation for a monovalent anion (Eq. 3). The GHK-fit (see Fig. 1) indicates that $[Cl^-]_c$ = 34 mM and V_c = −31.5 mV with a GHK-permeability, $P_{Cl} = 1.61 \cdot 10^{-14}$ cm$^3 \cdot$ s^{-1}. This permeability indicates a fairly small limiting conductance, $\gamma_{125/125}$ = 7.7 pS, and a physiological conductance at the reversal potential of no more than γ_{rev} = 3.7 pS (Eqs. 4 and 5, respectively).

In nine out of eleven cell-attached patches containing the small Cl^--channel the *i/V*-relationship could be fitted with Eq. 3 with reasonable values for $[Cl^-]_c$. The limiting conductance of these nine channels was $\gamma_{125/125} = 10.0 \pm 1.2$ pS (mean ± SEM, n = 9) with a conductance at the reversal potential, $\gamma_{rev} = 5.8 \pm 0.5$ pS. These fits were obtained with a reversal potential, $-V_{p,\,rev} = 1.7 \pm 1.2$ mV, an intracellular concentration, $[Cl^-]_c = 38.4 \pm 3.9$ mM, and an intracellular potential, V_c = -33.2 ± 2.5 mV. In two previous studies of toad skin the intracellular Cl^--concentration in MR-cells in situ was estimated to be ~20 mM (from cell volume decrease associated with depletion of the intracellular Cl^- pool, Larsen et al., 1987) and ~25 mM (by x-ray microprobe analysis, Rick et al., 1980), respectively. The somewhat higher concentration in isolated cells (38 mM) indicates a smaller membrane potential of these cells as compared to MR-cells in situ.

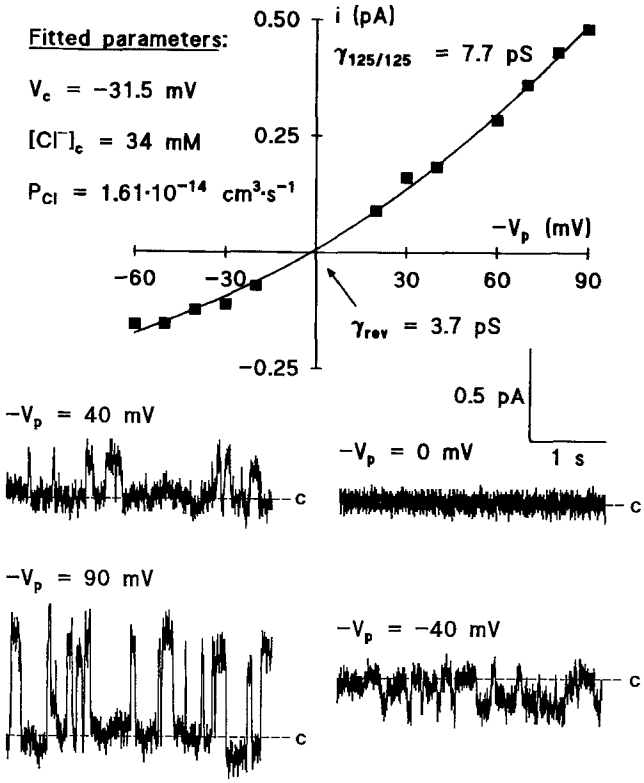

FIGURE 1. Cell-attached recordings of a small channel from an apical membrane-patch on a MR-cell. Modified Ringer in pipette and bath with $[Cl^-]$ = 125 mM. Shown are four recordings at identical gain and time scale. The closed level (baseline) is marked by a *c*. Pipette-potentials ($-V_p$) are indicated above traces. The *i/V*-relationship was obtained from means of Gaussian fits to all-points histograms taken at different potentials. The full line is fit of Eq. 3 with the parameters shown. From the estimated permeability, Eq. 4 provides the upper limit conductance, $\gamma_{125/125}$ = 7.7 pS, and Eq. 5 provides the conductance at the reversal potential, γ_{rev} = 3.7 pS. Currents were filtered at 200 Hz (−3 dB) and digitized at 2 kHz.

Inside-out configuration. The small apical channels were active in inside-out configuration as well, both with 4 mM Ca^{2+} (modified Ringer) and when the 100 nM free-Ca^{2+} solution superfused the cytoplasmic side of the membrane (see *Solutions*). For verifying Cl^- selectivity of the small channel, excised patches were perfused with a solution with a lower $[Cl^-]$. The patch in Fig. 2 was first observed under symmetrical conditions (125 mM Cl^- on both sides), where a number of small linear channels were active, each with a conductance of 8.4 pS (slope of the regression-line) and a reversal potential close to 0 mV. Perfusing the patch locally with 25 mM-Cl^- displaced the reversal potential to the left, i.e., towards the new E_{Cl}. At the same time, the *i/V*-relationship became nonlinear and could now be fitted

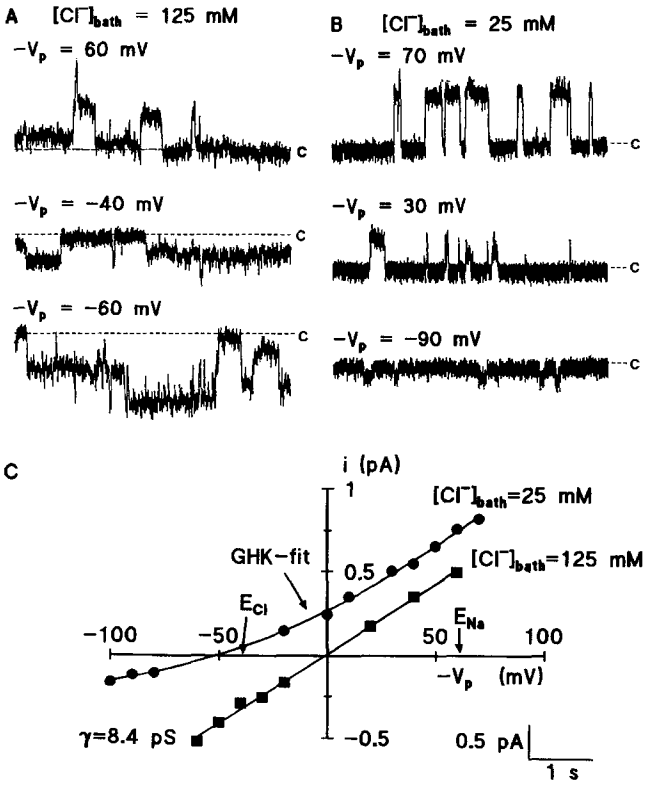

FIGURE 2. Current recordings of an excised inside-out membrane-patch containing several small channels. (*A*) Patch-recordings at different pipette-potentials with bath-[Cl^-] = 125 mM and pipette-[Cl^-] = 125 mM. (*B*) Recordings of the same patch after substitution of the bath for a solution with bath-[Cl^-] = 25 mM and free-[Ca^{2+}] = 100 nM. (*C*) *i/V*-relationships for the two conditions: (■) Bath-[Cl^-] = 125 mM. The full line is linear regression and the conductance (γ) is the slope of the regression-line. (●) Bath-[Cl^-] = 25 mM. Nernst potentials for Cl^- and Na^+ are indicated. The full line is fit of Eq. 3 with fixed concentrations at both sides and with $V_M = -V_p + V_{off}$. Parameters: V_{off} = 9.8 mV, P_{Cl} = 2.1×10^{-14} cm^3 s^{-1}, $\gamma_{125/125}$ = 10.0 pS (Eq. 4). The offset potential indicates that the reversal potential was estimated to the left of E_{Cl} (see text).

with Eq. 3 with the Cl^- concentrations on the two sides of the channel being fixed to their known values and allowing P_{Cl} and a potential-offset (V_{off}) to vary.

Channels resolved in 11 patches in symmetrical 125 mM Cl^- solutions all exhibited linear *i/V*-relationships with a mean-slope indicating a conductance of 7.1 ± 0.5 pS (n = 11). When the bath was exchanged for the perfusion solution with [Cl^-] = 25 mM, the reversal potential shifted from 0.22 ± 1.31 to −43.8 ± 2.7 mV. The estimated liquid junction potential between the two bath solutions was −2.7 mV (Table I), so that the current flowing in a Cl^- selective channel is expected to reverse at, $-V_p = E_{Cl} - V_{2,1} = -38$ mV. Thus, no permeability for gluconate$^-$/Na^+ could be detected. The mean reversal potential of −44 mV, instead of −38 mV, is possibly due to the fact that the reversal potential for some channels was estimated by extrapolation using Eq. 3.

Occasionally, even smaller channels were resolved. In Fig. 3 are shown recordings from an inside-out patch (125 mM Cl^- on both sides) where the current through a very small channel (γ = 1.9 pS) is superimposed on the baseline and the current through a 7.7-pS channel. The chloride selectivity of this small channel was confirmed subsequently by perfusing the channel's cytosolic side with 25 mM Cl^-.

Activity and kinetics in cell-attached patches. Among patches from different cells, the electrical activity of the small 7-pS Cl^- channel was extremely variable. However, in no case could a potential-dependence of open probability be detected (within ±60 mV). The kinetics of individual channels were hard to study, since, usually, several channels were present in the same patch. In three patches with apparently only a single active channel, two different gating modes were encountered (Fig. 4). One gating mode (1 patch) was characterized by two closed time-constants and a single open time-constant giving rise to a "bursting" activity, see Fig. 4 *A*. The other gating mode (2 patches) was characterized by a single closed time-constant, thus, apparently, conforming to a simpler two-state kinetic scheme (Fig. 4 *B*). Since most seals were short-lived, however, the existence of more time-constants than described above can not be ruled out.

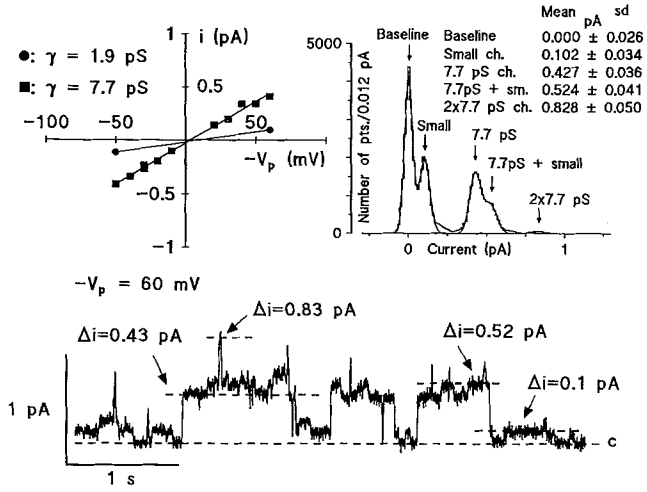

FIGURE 3. Recording of an inside-out patch with bath-[Cl^-] = pipette-[Cl^-] = 125 mM. (*Bottom*) Current-recording at $-V_p$ = 60 mV showing transitions of different magnitudes, indicating more than one conductance-level in the patch. (*Upper right*) All-points current amplitude histogram at $-V_p$ = 60 mV. The sum of 5 fitted Gaussian distributions is shown superimposed on the histogram. The current through a small channel resulted in a single Gaussian distribution (*Small*) when opening alone, and another (*7.7pS + sm.*) when opening together with the larger channel. (*Upper left*) *i/V*-curve of the larger (■) and the small (●) channel. The small channel could only be resolved with a driving force of ±60 mV. Conductances were calculated as the slope of the regression line.

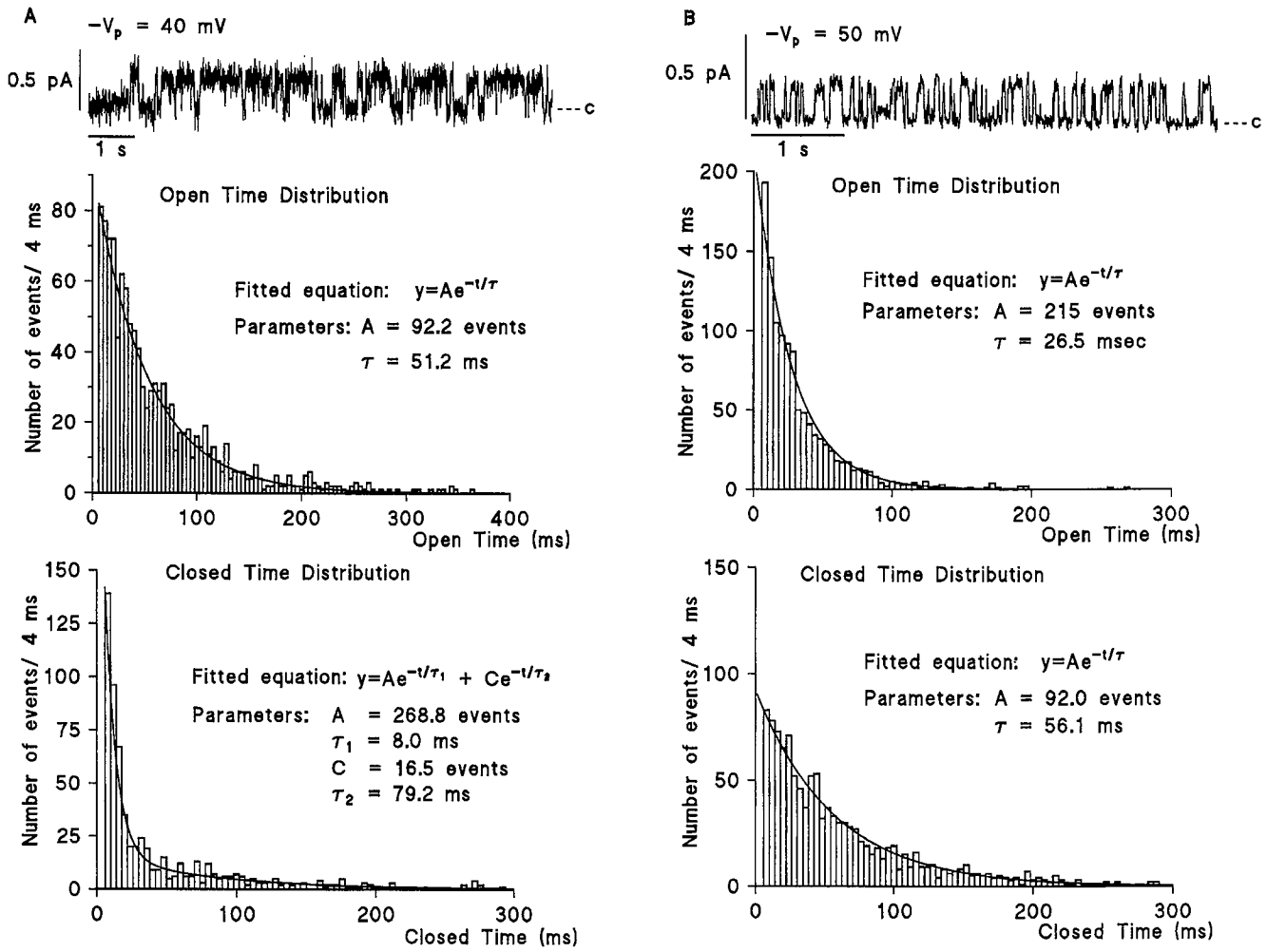

FIGURE 4. Two different gating modes of the small channel in single-channel patches. (*A*). (*Top*) Current-recordings of a cell-attached patch at $-V_p$ = 40 mV. Channel transitions were detected using two thresholds, corresponding to openings and closings, respectively. A minimum time-resolution of 4 ms was superimposed (Colquhoun and Sigworth, 1983). (*Middle*) The open time distribution. The histogram could be fitted with a single exponential, giving a mean open time of 51.2 ms. (*Bottom*) The closed time distribution. The histogram shows biexponential form and could be fitted with a sum of two exponentials with time constants τ_1 = 8 ms and τ_2 = 79 ms. (*B*). (*Top*) Current recordings of a cell-attached patch at $-V_p$ = 50 mV. (*Middle*) Open time distribution modified to a time resolution of 4 ms. The histogram could be fitted by a single exponential with τ= 26.5 ms. (*Bottom*) The closed time distribution was also mono-exponential, in this case with τ = 56.1 ms.

Effect of ATP and cAMP. After excision of the patch from the cell, the small channel exhibited variable levels of activity, and in eight out of nine excised patches the activity declined over the course of 5–18 min after excision. Apparently, this decline in activity was not affected by the addition of 3 mM ATP to the cytosolic side of the patch (bath). However, in all cases the rundown was so slow that the activity was not entirely lost within the lifetime of the patch.

The transepithelial Cl^- conductance of amphibian skin is regulated by cAMP (Kristensen, 1983; Nagel & Van Driessche, 1992; Willumsen et al., 1992; Katz and Nagel, 1995) and we therefore investigated whether the small channel could be activated by cAMP. Forskolin (12–25 μM) was ineffective in activating channels in silent cell-attached patches (n = 11, not shown). However, after pre-exposure for 5–60 min of the cells to forskolin, the fraction of patches containing the small channel increased from 23% (n = 155 patches) to 42% (n = 24 patches). To further investigate this point, we added the catalytic subunit of PKA to the cytoplasmic face of the membrane of inside-out patches. Due to the short life time of patches (MATERIALS AND METHODS), this was a very hard experiment to perform, thus in only 2 patches with spontaneous channel activity did the seal last long enough for the activity to be evaluated both with and without PKA. In both cases, the activity was increased after PKA addition. Fig. 5 shows an experiment where small channels in an inside-out patch were activated after the addition of PKA. Subsequent

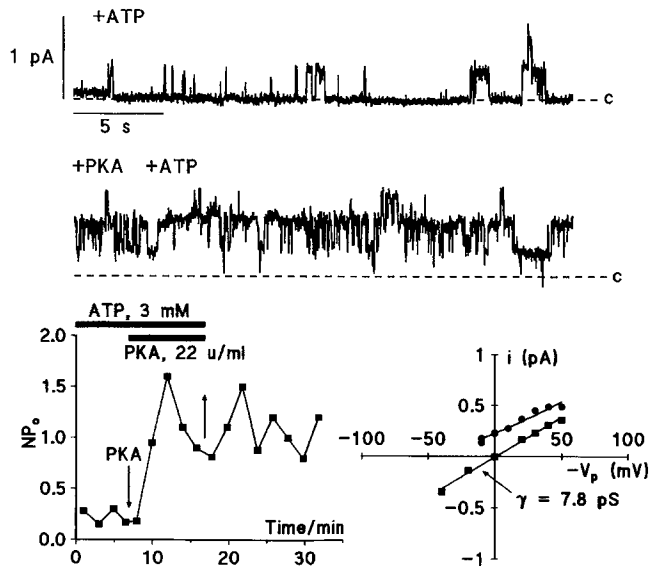

FIGURE 5. Current-recordings from an excised inside-out patch. (*Bottom right*) *i/V*-relationships with bath-[Cl^-] = 125 (■) and 25 mM (●), respectively, showing Cl^- selectivity of the channels. The conductance in symmetrical 125 mM Cl^- was 7.8 pS. Top traces were obtained at $-V_p$ = 20 mV with bath-[Cl^-] = 25 mM. The upper trace showed low activity with ATP (3 mM) in the bath. After addition of the catalytic subunit of protein kinase A (*PKA*, 22 U/ml) to the bath, with a delay of ~3 min, channels activated. (*Bottom left*) Activity measured in ~2 min (nonoverlapping) time intervals and displayed as a function of the mid-time of each interval. Channel activity increased after PKA-addition and stayed high even after perfusion with fresh Ringer with bath-[Cl^-] = 25 mM and no ATP (or PKA).

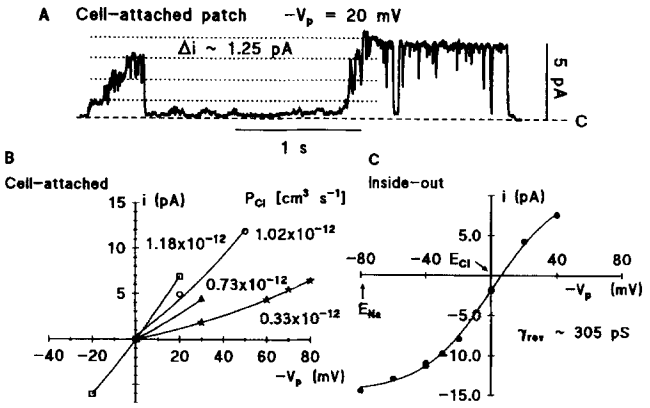

FIGURE 6. (*A*). Current-trace of a cell-attached patch at $-V_p$ = 20 mV obtained with bath-[Cl^-] = pipette-[Cl^-] = 125 mM. Notice the staircase-like partial opening of the channel lasting several hundred milliseconds, followed by a full opening. The (tentative) levels indicated correspond to one quarter of the full amplitude. (*B*). *i/V*-relationships for giant Cl^--channels from 4 cell-attached patches. Each relationship is fitted by Eq. 3 (the point [$-V_p$, *i*] = [0, 0] was included in the fit) and permeabilities, P_{Cl}, are given. (*C*). *i/V*-relationship for a giant channel resolved in an inside-out patch with bath-[Cl^-] = pipette-[Cl^-] = 125 mM; bath-[Na^+] = 116 mM, pipette-[Na^+] = 5.2 mM. Equilibrium-potentials for Cl^- (E_{Cl}) and Na^+ (E_{Na}) are indicated.

wash with ATP- and PKA-free solution did not inactivate the channels. This result is possibly related to the above observation of high activity of channels in inside-out patches in the absence of ATP. Accordingly the MR-cell channel is much less sensitive to ATP-free solutions than another cAMP regulated Cl^- channel, i.e., the cystic fibrosis transmembrane conductance regulator (CFTR; Anderson et al., 1991; Baukrowitz et al., 1994; Hwang et al., 1994). In three inside-out patches where spontaneous channel activity was not present, addition of PKA failed to activate any channels.

Giant Chloride Channels (3% of Patches)

In a few apical membrane patches we resolved Cl^- channels with a very high unitary conductance ($\gamma_{125/125}$ > 120 pS). The gating of these channels was characterized by complicated openings and closings that occurred in multiple steps or as single transitions of full amplitude (Fig. 6). When resolved in cell-attached patches, the channels exhibited GHK-rectification (Fig. 6). However, the estimated permeabilities were very variable indicating limiting conductances ranging from 150 to 550 pS. Chloride selectivity was confirmed from an inside-out patch resolved with NMDG-Cl in the pipette (Fig. 6). Under these conditions the channel reversed at 6 mV. According to our measurements of the liquid junction potential (−4.4 mV, Table I), the above reversal potential is comparable to the theoretical reversal potential of a Cl^--selective channel ($-V_p = -V_{LJ}$ = 4.4 mV). In cell-attached membrane-patches sustained activity was only seen at positive potentials (depolarization). Such activation of a giant channel is shown in Fig. 7, where the channel, in response to a 20-mV depolarization, activated together with a number of smaller

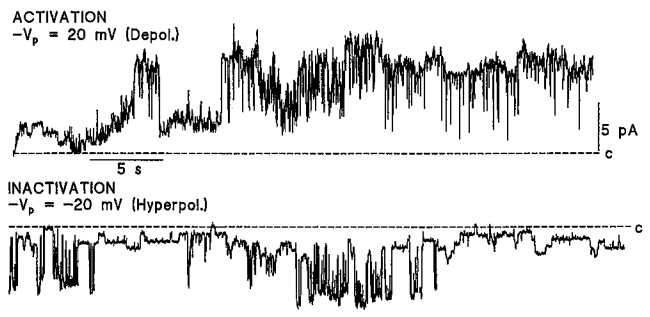

FIGURE 7. Current recordings from a cell-attached apical membrane-patch obtained with bath-[Cl^-] = pipette-[Cl^-] = 125 mM showing activation and inactivation of a giant Cl^--channel. (*Top*) Current trace at $-V_p$ = 20 mV obtained immediately after changing the potential from 0 mV. Several small and a giant channel activate gradually. (*Bottom*) Current trace at $-V_p$ = −20 mV obtained immediately after changing from 20 mV. The giant channel inactivated and stayed closed hereafter (not shown). Several smaller channels exhibited sustained activity.

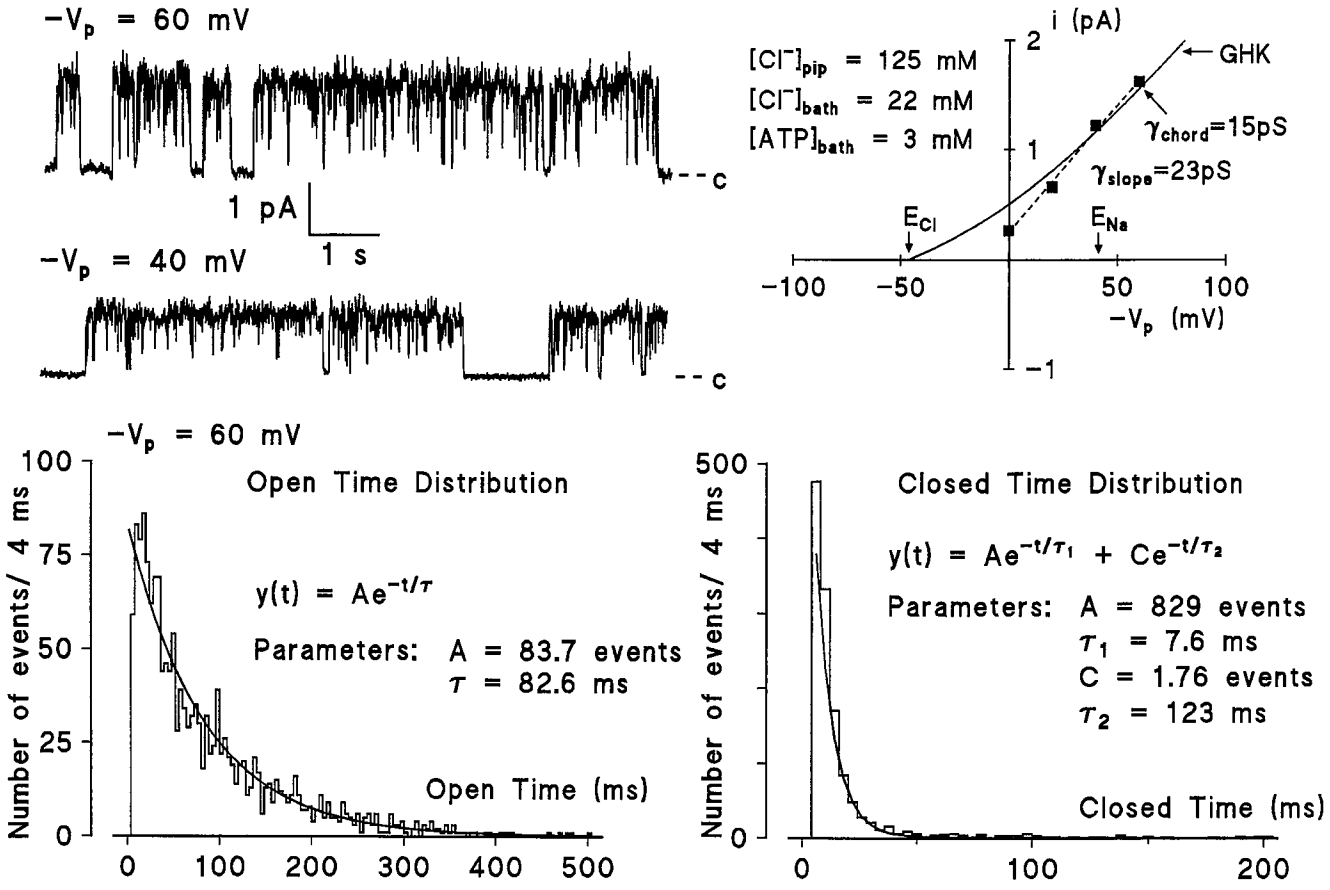

FIGURE 8. An intermediate conductance Cl^--channel in an inside-out patch. Pipette-[Cl^-] = 125 mM, bath-[Cl^-] = 22 mM, bath-[Mg-ATP] = 3 mM. The channel activated in inside-out configuration after exchange of the bath solution. (*Top left*) Current recordings at two potentials filtered at 200 Hz and digitized at 1 kHz. Note the distinct bursts of activity. (*Top right*) *i/V*-relationship of the channel. The *i/V*-relationship was linear despite the skewed concentrations. The slope of the regression-line (γ_{slope}) was 23 pS. The chord conductance at 60 mV ($-V_p$) was 15 pS. Shown is the best fit of Eq. 3 fixed to pass through E_{Cl}. (*Bottom left*) Open time distribution at $-V_p$ = 60 mV. Minimum time resolution = 4 ms. The histogram shows monoexponential form with τ = 82.6 ms. (*Bottom right*) Closed time distribution. Most closings are brief (τ_1 = 7.62 ms), however clearly longer closings do appear (compare *top left*). The second exponential (τ_2 = 123 ms) is not well identified.

channels. The recordings in Fig. 7 also show that after hyperpolarization the giant channel lost its electrical activity whereas a number of smaller channels continued being active.

Intermediate Chloride Channels (10% of Patches)

Different Cl^- channels of intermediate conductances were resolved. Among the most frequent (~5%) were channels exhibiting openings occurring in distinct "bursts" separated by longer closings. The current-voltage relationships in this group were linear, or slightly outwardly rectifying, with a slope conductance ranging from 14 to 53 pS (mean ± SEM = 29.8 ± 4.3 pS, n = 9). Recordings from such a channel are shown in Fig. 8. In this inside-out patch the channel became active after exchange of the bath with a Tris-solution with 22 mM Cl^- and 3 mM ATP. Channel transitions of positive amplitude occurred at 0 mV. Since only two permeant ions (Na^+ and Cl^-) were present of which only Cl^- had a reversal potential <0 mV, this verified Cl^- selectivity of the channel. The *i/V*-relationship was linear under these asymmetric conditions with a slope conductance of 23 pS. Thus, the channel might be rectifying the currents slightly in the outward direction as compared to simple electrodiffusion (Eq. 3). The distribution of open-times showed single-exponential form with a time-constant of 83 ms, see Fig. 8. The closed-time distribution was dominated by fast closings (τ = 7.6 ms). As can be seen from the traces in Fig. 8, a number of longer closings were also apparent. However, in the fit of a sum of two exponentials to the event-distribution histogram, the second time-constant (123 ms in Fig. 8) is poorly determined.

Occasionally, we resolved channels of intermediate conductance with a voltage-dependent open-probability. The conductance of these channels ranged from 10 to 27 pS (n = 4). The channel in Fig. 9 exhibited

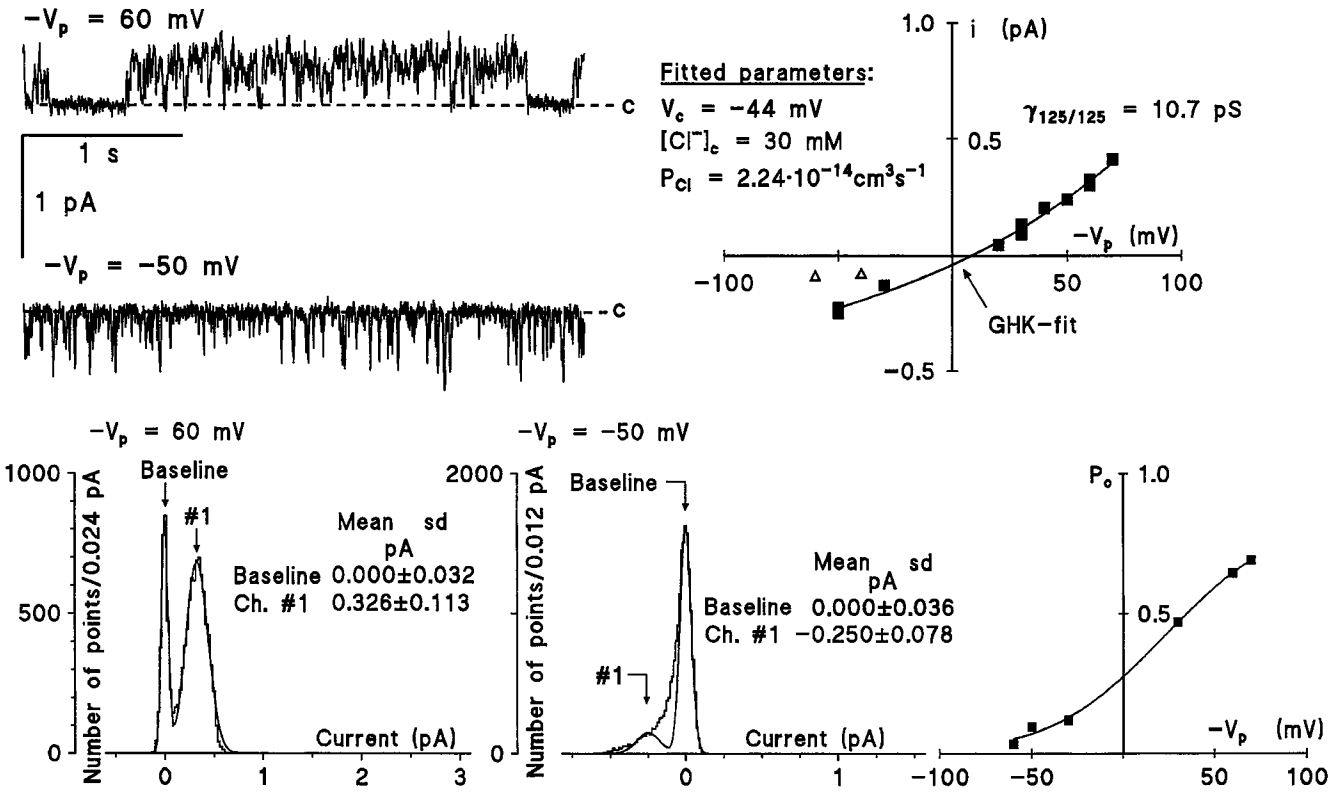

FIGURE 9. (*Top left*) Current recordings of a single channel in a cell-attached patch. The channel exhibits longer openings at potentials >0 mV and brief flickering at <0 mV. (*Top right*) *i/V*-relationship of the channel. Points at $-V_p < 0$ mV are considered tentative. Filled rectangles are included in the fit of Eq. 3 assuming electrodiffusion of Cl^- and resulting in the parameters shown. The upper limit conductance ($\gamma_{125/125}$) is calculated as 10.7 pS. (*Bottom left and middle*) All-points current amplitude histograms showing a distinct, well defined open-state at 60 mV and a poorly defined open-state at −50 mV. (*Bottom right*) Estimated relationship of P_o versus $-V_p$.

longer, noisy openings at positive $-V_p$, and partly unresolved flickers at $-V_p < 0$. For $-V_p > 0$, the current amplitude histogram resolved the open state of the channel as a broad Gaussian, whereas the flickers observed at $-V_p < 0$ resulted in a tail on the distribution with the open state being unresolved. It can also be seen (Fig. 9) that despite the fact that the measurements at negative $-V_p$ must be very tentative, the *i/V*-relationship could be fitted with Eq. 3 with reasonable parameters for a Cl^--channel in an MR-cell. This is preliminary evidence for a Cl^--selective channel. However, since this channel was not resolved under asymmetrical conditions, Cl^- selectivity was not verified directly. The conductance of this channel was not much different from that of the "small linear Cl^- channels" described above. However, the channel exhibited a markedly different kinetics and voltage dependence. The estimated ($-V_p$, P_o)-relationship shown in Fig. 9 indicates channel activation in response to depolarization.

Chloride Channels of Unresolvable Kinetics (4% of Patches)

As exemplified by the records shown in Fig. 10, some patches could be quite noisy. Since all-points histograms failed to resolve single current levels (not shown), one would be tempted to discontinue further analysis. However, when the bath solution of inside-out patches was exchanged for one with a lower Cl^--concentration, it turned out that the potential at which noise was at its minimum shifted towards the new E_{Cl} ($-V_{2,1}$). This would be expected if the noise is generated by random opening and closing of Cl^--channels. For this case the variance of current fluctuations (σ^2) is given by:

$$\sigma^2 = \gamma^2 \cdot \{-V_p - (E_{Cl} - V_{2,1})\}^2 \cdot N \cdot P_o \cdot (1 - P_o) + \sigma_{leak}^2, \quad (6)$$

where, σ_{leak}^2 is the variance contributed from the current through the seal, and the first term is the variance of current through ion channels (assuming a homogeneous population of N channels). Clearly, when $-V_p = E_{Cl} - V_{2,1}$, the variance of the first term is zero. Since the variance through the leak is probably also voltage dependent, the total current variance is expected to reach a minimum somewhere between 0 and $E_{Cl} - V_{2,1}$. For investigating this point, the patch-currents recorded at different potentials were redigitized using the SPAN-software, and the variance of the current segments subsequently calculated. The result shown in Fig. 10 indicates that the variance, indeed, was at its

minimum near $E_{Cl} - V_{2,1}$. This result confirms Cl^- selectivity of the noise-source, since a nonselective leak would have a noise minimum near 0 mV. The *i/V*-relationship of the patch was constructed by pulsing for 200 ms the potential to different values within ±100 mV. The resulting currents (Fig. 10) are the sum of the leak current (since leakage subtraction was not used) and current through the Cl^--selective channels. By linear regression at $-V_p < 0$ mV (thus close to E_{Cl}), the patch resistance was found to be >10 GΩ. At $V_p > 0$mV the current exhibited outward rectification in excess of linear regression as expected if the current is the sum of a leakage current and the current through a population of GHK-rectifying channels.

It should be noted that channels with similar unresolvable kinetics might have been more frequent than indicated above (4%) since for cases where a patch was studied under symmetrical conditions, only, unresolvable channel activity would be mistaken for a bad seal.

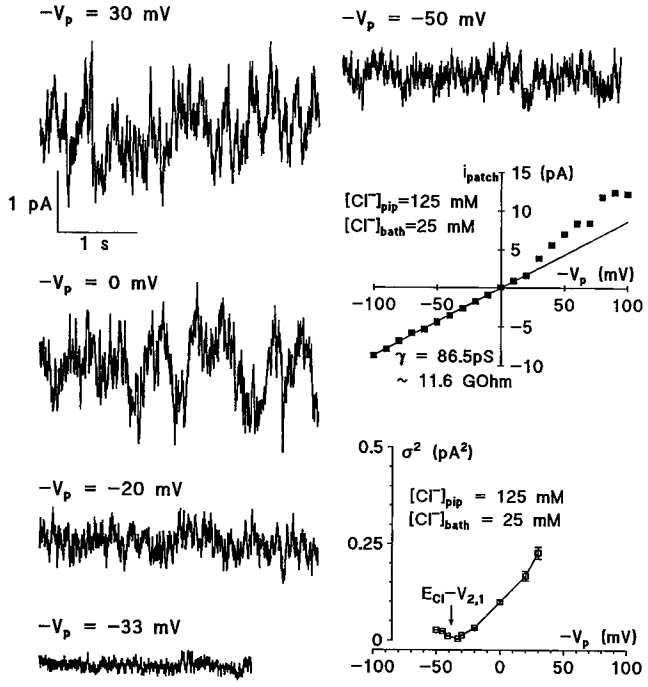

FIGURE 10. Example of a patch with unresolved kinetics of Cl^--selective channels. Shown are recordings of an inside-out patch with pipette-$[Cl^-]$ = 125 mM and bath-$[Cl^-]$ = 25 mM, thus $E_{Cl}-V_p$ is ~−38 mV. The current traces exhibited marked flickering and unresolved levels even at 0 mV pipette-potential. The $i_{patch}/-V_p$ relationship in the interval [−100 mV; 100 mV] went through (0, 0) (because leakage subtraction was not used) and exhibited outward rectification in excess of linear regression at positive $-V_p$. Linear regression to points <0mV shows that the seal resistance is at least 10 GΩ. The variance (σ^2) was calculated by digitizing currents at 1 kHz after low-pass filtering at 500 Hz (−3 dB) using SPAN software. The currents were divided into blocks of 1,024 points, and the variance was calculated for each block. Shown is the mean ± SEM of the variance at each pipette-potential. The plot of σ^2 versus $-V_p$ has a minimum near $E_{Cl}-V_{2,1}$ demonstrating Cl^- selectivity of the channels generating the current fluctuations.

DISCUSSION

In the present study we have identified Cl^- channels in the apical membrane of mitochondria-rich cells isolated from toad skin. This finding provides direct evidence that MR-cells, as opposed to the more abundant principal cells (Willumsen and Larsen, 1986), are able to conduct chloride passively across the apical membrane, thus corroborating macroscopic findings of an apical Cl^- conductance in MR-cells in situ. Furthermore, features predicted from macroscopic studies, i.e., activation of channel gating by membrane depolarization and internal exposure to PKA, respectively, were found among Cl^- channels resolved in apical membrane patches. The population of apical Cl^- channels was quite heterogeneous with respect to single channel conductances and kinetics of channel gating which may reflect participation of several different ion channels in the process of Cl^- absorption.

Frequency and Heterogeneity of Apical Chloride Channels in MR-Cells

Voltage-activated Cl^- channels were resolved in a minority of patches, only, and in more than half of the patches electrically active ion channels were not detected at all (Table II). It is clearly indicated, then, that although single populations of Cl^- channels were found which shared features with one or more macroscopic properties of the skin, the observed channel activity seems not to match, quantitatively, previously investigated macroscopic tissue conductances. We can suggest several reasons which may all have contributed to the low-frequency occurrence of apical Cl^- channels: (*a*) The cell-isolation procedure and subsequent establishment of patch-recording conditions may have resulted in enzymatic and mechanical impairments, respectively, of the cell membrane ion conductances. In agreement with this notion, whole-cell currents of our preparation also indicated that the MR-cell membrane's Cl^- conductance is far too small for accounting for the MR-cell currents estimated in Ussing-chamber experiments (Larsen and Harvey, 1994). (*b*) Functional heterogeneity of MR-cells has been demonstrated in macroscopic investigations of MR-cells in situ. Using vibrating voltage-electrodes Foskett and Ussing (1986) found current-profiles above 13 out of 23 MR-cells, whereas Katz and Scheffey (1986) reported on profiles above 30–90% of MR-cells in different preparations.[2]

[2]For improving the resolution of the method, these two studies with the vibrating electrode used preparations with a reduced number of MR-cells obtained from animals preadapted to a solution of high [NaCl].

Rick (1994) confirmed that in frog skin two populations of MR-cells could be distinguished, one of which took up Br^- from the outside solution whereas the other did not. The existence of MR-cells without an apical Cl^- conductance might indicate that some MR-cells express other functions than passive Cl^- absorption, such as acid or base secretion which have been associated with α-type and β-type intercalated cells, respectively, of distal renal epithelia (Steinmetz, 1986). (*c*) The patches that were obtained on MR-cells might not be representative of the entire apical membrane area of the population of MR-cells. This is because the process of successful seal formation might select for cells, or areas of the cell membrane, with a low channel density. While this is a problem that in principle applies to all single-channel patch-clamp investigations, the low frequency of seal formation in the present study makes it especially pertinent. (*d*) The MR-cells of the present preparation retain their structural polarity and appear flask shaped in isolation. However, it is a question of whether the functional polarity is also retained or whether channel proteins are free to diffuse laterally between apical and basolateral membrane areas. There is clearly a need to investigate the functional polarity of the isolated MR-cells.

In conclusion, there seem to be good reasons for exploring whether isolation and recording procedures impair the native membrane ion conductances. Furthermore, reasons for finding a large fraction of isolated MR cells with no apical Cl^- conductance also have to be investigated. At the present stage of our analysis, therefore, it is not possible quantitatively to bridge the description of the macroscopic Cl^- conductance of the intact tissue with that of single Cl^- channels of isolated MR cells.

The Small Conductance Chloride Channel

The most frequently encountered ion channel in apical membrane-patches was a small Cl^- channel with a linear *i/V*-relationship and a unitary conductance of 7 pS when observed under conditions of symmetrical 125-mM Cl^- (Figs. 1 and 2; Table II). Thus, in cell-attached and in excised inside-out patches, studied with different or similar Cl^- concentrations on the two sides of the membrane, single channel *i/V*-relationships were well described by electrodiffusion of Cl^- (Eq. 3). Furthermore, we succeeded in studying the same channel at different concentrations on the cytosolic side of the patch and demonstrated that the reversal potential of the channel current was governed by the equilibrium potential for Cl^-. Taken together, these observations allow us to conclude that a population of MR-cells harbors small Cl^--selective ion channels. The channel exhibited slow run-down in excised configuration and was active with both 4 mM and 100 nM free Ca^{2+} on the cytoplasmic side. The kinetics were characterized by one open-state time-constant and one or two closed-state time-constants (Fig. 4). The frequency of the channel increased by preincubation of the cells in forskolin which by activating a membrane bound adenyl cyclase is supposed to raise cytoplasmic [cAMP]. In excised inside-out membrane-patches the channel could be activated by the catalytic subunit of cAMP-dependent protein kinase (PKA; Fig. 5).

The above list of properties compares well with features of similar small Cl^- channels encountered in the apical membrane of several ion-transporting epithelia, for instance the human airways (Haws et al., 1992; 1994), pancreatic duct (Gray et al., 1988; 1989), colon cell lines (Tabcharani et al., 1990), *Necturus* gallbladder (Copello et al., 1993), and shark rectal gland (Gögelein et al., 1987; Devor et al., 1995). The appearance of these phosphorylation-activated Cl^- channels is generally ascribed to the expression of the CFTR-gene. However, compared to CFTR some differences must be noted. The small channel encountered here was quite active in inside-out patches even when excised into ATP-free solutions. Even though run-down was generally observed, activity was never completely lost. In the experiment in Fig. 5, channel activity continued for 15 min after wash with an ATP-free solution. Thus, the dependence of ATP is much less pronounced than generally reported for CFTR (Anderson et al., 1991; Baukrowitz et al., 1994). It is important to note, though, that the experiments were all done at room temperature (the relevant temperature when studying amphibian ion channels), and, therefore, comparison to mammalian CFTR studied at 37°C is difficult. For example, CFTR expressed in IEC-CF7 cells remained active without ATP at room temperature, but exhibited rapid run-down at 37°C (Bijman et al., 1993).

It is interesting that the small channel was found in the apical membrane of the same cell type as a channel type exhibiting unresolved kinetics. Such gating has been reported for cAMP-activated channels of HT-29 cells (Kunzelmann et al., 1992), a bronchial cell-line (Kunzelmann et al., 1994) and, recently, in *Sf*9-cells expressing CFTR using the baculovirus *Autographa californica* transient expression-system (Larsen et al., 1996).

The identification of cAMP-activated Cl^- channels in the apical membrane of MR-cells points to a role for these cells in the β-adrenergically controlled and cAMP-mediated Cl^- conductance previously studied in intact epithelia (Nagel and Van Driessche, 1992; Willumsen et al., 1992; Katz and Nagel, 1995). In rabbit cortical collecting tubule, another heterocellular absorptive epithelium, catecholamines (isoproterenol and L-norepinephrine), have also been shown to stimulate a Cl^- conductance (Iino et al., 1981; Nagy et al., 1994). It is especially interesting that this effect is exerted by

isoproterenol which specifically raises cAMP in the intercalated cells. Whole-cell patch clamp studies of intercalated cells in culture verified that a membrane Cl^--current is activated by cAMP (Ikeda et al., 1993; Dietl et al., 1992). Thus, we might hypothesize that the mediation of a cAMP-induced Cl^- conductance is yet another shared feature between mitochondria-rich cells of amphibian skin and intercalated cells of the vertebrate nephron.

Giant and Intermediate Chloride Channels

By its voltage dependence and single channel conductance, the giant apical Cl^- channel shares properties with a Cl^- channel characterized in a recent whole-cell study of Cl^- current fluctuations (Larsen and Harvey, 1994). Our single channel recordings showed that this channel exhibits very complex openings, characterized by several substates and a large unitary conductance, >125 pS (Figs. 6 and 7). It is possible, therefore, that the large conductance levels of this population of channels results from the coordinated activity of several membrane pores of lower unitary conductances. Mechanical impairment of these putative "clusters" by the process of seal formation might then explain the low frequency of occurrence in single-channel patches. This is, however, pure speculation. Chloride channels with similar large conductances have previously been reported from the amphibian kidney A6-cell line (Nelson et al., 1984), cultured cells from rabbit cortical collecting duct (Light et al., 1990; Schwiebert et al., 1990), alveolar cells (Kemp et al., 1993), and bovine trachea (Duszyk et al., 1995). It has been suggested that the function of this channel in the apical membrane of the cortical collecting duct is associated with cell volume-regulation (Schwiebert et al., 1992). Such a function does not compare with its activation by membrane depolarization in toad skin MR-cells which with an inwardly directed driving force on the chloride ions would result in Cl^- uptake and further volume expansion, rather than a regulatory volume decrease.

The population of intermediate channels was in itself heterogeneous and is not easy to compare with other findings. We find, however, that the coexistence of the small linear Cl^- channel together with a larger (often outwardly rectifying) Cl^- channel is a general feature of many epithelia as for example, pancreatic duct (Gray et al., 1989), hen colon (Fischer et al., 1991), shark rectal gland (Greger et al., 1987), and human airways (reviewed by Anderson et al., 1992). These tissues are characterized by coexpression of CFTR and a larger channel. Upon activation, both channel types are supposed to secrete Cl^-. The findings of similar Cl^- channels in the apical membrane of the toad skin points to a role of these channels in absorbing epithelia as well.

This study was supported by the Danish Natural Science Research Council (grant no. 11-0971) and the Carlsberg and Novo Nordisk Foundations. J.B. Sørensen was awarded a Novo Nordisk Student Scholarship and a grant from the Royal Danish Academy of Sciences and Letters.

Original version received 20 May 1996 and accepted version received 20 August 1996.

REFERENCES

Anderson, M.P., H.A. Berger, D.P. Rich, R.J. Gregory, A.E. Smith, and M.J. Welsh. 1991. Nucleoside triphosphates are required to open the CFTR chloride channel. *Cell.* 67:775–784.

Anderson, M.P., D.N. Sheppard, H.A. Berger, and M.J. Welsh. 1992. Chloride channels in the apical membrane of normal and cystic fibrosis airway and intestinal epithelia. *Am. J. Physiol.* 263: L1–L14.

Baukrowitz, T., T.-C. Hwang, A.C. Nairn, and D.C. Gadsby. 1994. Coupling of CFTR Cl^- channel gating to an ATP hydrolysis cycle. *Neuron.* 12:473–482.

Bijman, J., W. Dalemans, M. Kansen, J. Keulemans, E. Verbeek, A. Hoogeveen, H.D. Jonge, M. Wilke, D. Dreyer, J.-P. Lecocq, A. Pavirani, and B. Scholte. 1993. Low conductance chloride channels in IEC-6 and CF nasal cells expressing CFTR. *Am. J. Physiol.* 264:L229–L235.

Colquhoun D. and F.J. Sigworth. 1983. Fitting and statistical analysis of single-channel records. *In* Single-channel Recording. B. Sakmann and E. Neher, editors. Plenum Press, New York.

Copello, J., T.A. Heming, Y. Segal, and L. Reuss. 1993. cAMP-activated apical membrane chloride channels in *Necturus* gallbladder epithelium. Conductance, selectivity, and block. *J. Gen. Physiol.* 102:177–199.

Devor, D.C., J.N. Forrest, Jr., W.K. Suggs, and R.A. Frizzel. 1995. cAMP-activated Cl^- channels in primary cultures of spiny dogfish (*Squalus acanthias*) rectal gland. *Am. J. Physiol.* 268:C70–C79.

Devuyst, O., V. Beaujean, and J. Crabbé. 1991. Effects of environmental conditions on mitochondrial-rich cell density and chloride transport in toad skin. *Pflügers Arch.* 417:577–581.

Dietl, P., N. Kizer, and B.A. Stanton. 1992. Conductive properties of a rabbit cortical collective duct cell line: regulation by isoproterenol. *Am. J. Physiol.* 262:F578–F82.

Duszyk, M., D. Liu, B. Kamosinska, A.S. French, and S.F. Paul Man. 1995. Characterization and regulation of a chloride channel from bovine tracheal epithelium. *J. Physiol. (Lond.).* 489:81–93.

Ehrenfeld, J., I. Lacoste, and B.J. Harvey. 1989. The key role of the mitochondria-rich cells in Na^+ and H^+ transport across the frog skin epithelium. *Pflügers Arch.* 414:59–67.

Fischer, H., W. Kromer, and W. Clauss. 1991. Two types of chloride channels in hen colon epithelial cells identified by patch-clamp experiments. *J. Comp. Physiol.* 161:333–338.

Foskett, J.K., and H.H. Ussing. 1986. Localization of chloride conductance to mitochondria-rich cells in frog skin epithelium. *J. Membr. Biol.* 91:251–258.

Gögelein, H., E. Schlatter, and R. Greger. 1987. The "small" conductance chloride channel in the luminal membrane of the rectal gland of the dogfish (*Squalus acanthias*). *Pflügers Arch.* 409:122–125.

Goldman, D.E. 1943. Potential, impedance, and rectification in membranes. *J. Gen. Physiol.* 27:37–60.

Gray, M.A., J.R. Greenwell, and B.E. Argent. 1988. Secretin-regulated chloride channel on the apical plasma membrane of pancreatic duct cells. *J. Membr. Biol.* 105: 131–142.

Gray, M.A., A. Harris, L. Coleman, J.R. Greenwell, and B.E. Argent. 1989. Two types of chloride channel on duct cells cultured from human fetal pancreas. *Am. J. Physiol.* 257:C240–C251.

Greger, R., E. Schlatter, and H. Gögelein. 1987. Chloride channels in the luminal membrane of the rectal gland of the dogfish (*Squalus acanthias*). *Pflügers Arch.* 409:114–121.

Harvey, B.J. 1992. Energization of sodium absorption by the H-ATPase pump in mitochondria-rich cells of frog skin. *J. Exp. Biol.* 172: 289–309.

Haws, C., W.E. Finkbeiner, J.H. Widdicombe, and J.J. Wine. 1994. CFTR in Calu-3 human airway cells: channel properties and role in cAMP-activated Cl^- conductance. *Am. J. Physiol.* 266:L502– L512.

Haws, C., M.E. Krouse, Y. Xia, D.C. Gruenert, and J.J. Wine. 1992. CFTR channels in immortalized human airway cells. *Am. J. Physiol.* 263: L692–L707.

Hodgkin, A.L., and B. Katz. 1949. The effect of sodium ions on the electrical activity of the giant axon of the squid. *J. Physiol. (Lond.).* 102:37–77.

Hwang, T.-C., G. Nagel, A.C. Nairn, and D.C. Gadsby. 1994. Regulation of the gating of cystic fibrosis transmembrane conductance regulator Cl channels by phosphorylation and ATP hydrolysis. *Proc. Natl. Acad. Sci. USA.* 91:4698–4702.

Iino, Y., J.L. Troy, and B.M. Brenner. 1981. Effects of catecholamines on electrolyte transport in cortical collecting tubule. *J. Membr. Biol.* 61:67–73.

Ikeda, M., M. Iyori, K. Yoshitomi, M. Hayashi, M. Imai, T. Saruta, and K. Kurokawa. 1993. Isoproterenol stimulates Cl^- current by a Gs protein-mediated process in β-intercalated cells isolated from rabbit kidney. *J. Membr. Biol.* 136:231–241.

Katz, U., and S. Gabbay. 1988. Mitochondria-rich cells and carbonic anhydrase content of toad skin epithelium. *Cell Tissue Res.* 251: 425–431.

Katz, U., and W. Nagel. 1995. Effects of cyclic AMP and theophylline on chloride conductance across toad skin. *J. Physiol. (Lond.).* 489:105–114.

Katz, U., and C. Scheffey. 1986. The voltage-dependent chloride current conductance of toad skin is localized to mitochondria-rich cells. *Biochim. Biophys. Acta.* 861:480–482.

Kemp, P.J., G.G. MacGregor, and R.E. Olver. 1993. G protein-regulated large conductance chloride channels in freshly isolated fetal type II alveolar epithelial cells. *Am. J. Physiol.* 265:L323–L329.

Kristensen, P. 1978. Effect of amiloride on chloride transport across amphibian epithelia. *J. Membr. Biol.* 40:167–185.

Kristensen, P. 1981. Is chloride transfer in frog skin localized to a special cell type? *Acta Physiol. Scand.* 113:123–124.

Kristensen, P. 1983. Exchange diffusion, electrodiffusion and rectification in the chloride transport pathway of frog skin. *J. Membr. Biol.* 72:141–151.

Kunzelmann K., T. Koslowsky, T. Hug, D.C. Gruenert, and R. Greger. 1994. cAMP-dependent activation of ion conductances in bronchial epithelial cells. *Pflügers Arch.* 428:590–596.

Kunzelmann K., M. Grolik, R. Kubitz, and R. Greger. 1992. cAMP-dependent activation of small- conductance Cl^- channels in HT_{29} colon carcinoma cells. *Pflügers Arch.* 421:230–237.

Larsen, E.H. 1991. Chloride transport by high-resistance heterocellular epithelia. *Physiol. Rev.* 71:235–283.

Larsen, E.H., and B.J. Harvey. 1994. Chloride currents of single mitochondria-rich cells of toad skin epithelium. *J. Physiol. (Lond.).* 478:7–15.

Larsen, E.H., E.M. Price, S.E. Gabriel, M.J. Stutts, and R.C. Boucher. 1996. Clusters of Cl^- channels in CFTR-expressing *Sf*9 cells switch spontaneously between slow and fast gating modes. *Pflügers Arch.* 432:528–537.

Larsen, E.H., H.H. Ussing, and K.R. Spring. 1987. Ion transport by mitochondria-rich cells in toad skin. *J. Membr. Biol.* 99:25–40.

Larsen, E.H., N.J. Willumsen, and B.C. Christoffersen. 1992. Role of proton pump of mitochondria-rich cells for active transport of chloride ions in toad skin epithelium. *J. Physiol. (Lond.).* 450:203–216.

Light, D., E.M. Schwiebert, G. Fejes-Toth, A. Naray-Fejes-Toth, K.H. Karlson, F.V. McCann, and B.A. Stanton. 1990. Chloride channels in the apical membrane of cortical collecting duct cells. *Am. J. Physiol.* 258:F273–F280.

Nagel, W., and W. Van Driessche. 1992. Effect of forskolin on conductive anion pathways of toad skin. *Am. J. Physiol.* 263:C166–C171.

Nagy, E., A. Náray-Fejes-Tóth, and G. Fejes-Tóth. 1994. Vasopressin activates a chloride conductance in cultured cortical collecting duct cells. *Am. J. Physiol.* 267:F831–F838.

Neher, E. 1992. Correction for liquid junction potentials in patch clamp experiments. *Methods Enzymol.* 207:123–131.

Nelson, D., J.M. Tang, and L.G. Palmer. 1984. Single-channel recordings of apical membrane chloride conductance in A6 epithelial cells. *J. Membr. Biol.* 80:81–89.

Page, R.D., and L.W. Frazier 1987. Morphological changes in the skin of *Rana pipiens* in response to metabolic acidosis. *Proc. Soc. Exp. Biol. Med.* 184:416–422.

Rick, R. 1992. Intracellular ion concentrations in the isolated frog skin epithelium: Evidence for different types of mitochondria-rich cells. *J. Membr. Biol.* 127: 227–236.

Rick, R. 1994. Short-term bromide uptake in skins of *Rana pipiens*. *J. Membr. Biol.* 138:171–179.

Rick, R., A. Dörge, U. Katz, R. Bauer, and K. Thurau. 1980. The osmotic behavior of toad skin epithelium (*Bufo viridis*). *Pflügers Arch.* 385:1–10.

Schwiebert, E.M., K.H. Karlson, P.A. Friedman, P. Dietl, W.S. Spielman, and B.A. Stanton. 1992. Adenosine regulates a chloride channel via protein kinase C and a G protein in a rabbit cortical collecting duct cell line. *J. Clin. Invest.* 89:834–841.

Schwiebert, E.M., D.B. Light, G. Fejes-Toth, A. Naray-Fejes-Toth, and B.A. Stanton. 1990. A GTP-binding protein activates chloride channels in a renal epithelium. *J. Biol. Chem.* 265:7725–7728.

Steinmetz, P.R. 1986. Cellular organization of urinary acidification. *Am. J. Physiol.* 251:F173– F187.

Sten-Knudsen, O. 1978. Passive transport processes. *In* Membrane Transport in Biology: Concepts and Models. G. Giebisch, D.C. Tosteson, and H.H. Ussing, editors. Springer-Verlag, New York. 5–113.

Tabcharani, J.A., W. Low, D. Elie, and J.W. Hanrahan. 1990. Low conductance chloride channel activated by cAMP in the epithelial cell line T_{84}. *FEBS Lett.* 270:157–164.

Voûte, C.L., and W. Meier. 1978. The mitochondria-rich cell of frog skin as hormone-sensitive "shunt-path". *J. Membr. Biol.* 40:151–165.

Willumsen, N.J., and E.H. Larsen. 1986. Membrane potentials and intracellular Cl^- activity of toad skin epithelium in relation to activation and deactivation of the transepithelial Cl^- conductance. *J. Membr. Biol.* 94:173–190.

Willumsen, N.J., L. Vestergaard, and E.H. Larsen. 1992. Cyclic AMP- and β-agonist-activated chloride conductance of a toad skin epithelium. *J. Physiol. (Lond.).* 449:641–653.